physica status solidi b
www.pss-b.com

Electronic Dynamics in 2D Aperiodic Systems under Effect of Electric Field

*Renato F. Dutra, Demitry Messias, Caio V.C. Mendes, Adhemar Ranciaro Neto, Messias O. Sales, and Francisco A. B. F. de Moura**

On a square lattice with aperiodic hopping terms, the dynamics of an initially localized one electron wave-packet is investigated using a Taylor formalism to solve Schrödinger dynamic equation. The calculations suggest that a fast electron propagation (ballistic mode) is detected for a range of values of aperiodicity measure ν. When inserting static electric field effects in the model, the existence of an oscillatory behavior analogously to electronic dynamics in crystalline systems is verified (i.e., Bloch oscillations). The frequency and the the size of these oscillations are analyzed and the results are compared with the standard semi-classical approach used in crystalline lattices.

1. Introduction

Electronic propagation in quasi-crystals or aperiodic systems is a current theme with several theoretical and experimental investigation.[1–22] Das Sarma was the first to demonstrate that slowly varying deterministic potentials promote the emergence of extended states.[13,14] He and his coworkers initially considered an 1D model in which the potential energy at the site n is proportional to $\cos(\pi\alpha n^{\nu})$. In the most famous variant of that author's model, $\pi\alpha$ is a rational number and $\nu > 0$. This parameter (ν) characterizes either randomicity or periodicity of on-site potentials. For $0 < \nu < 1$, the diagonal potential is aperiodic; for $\nu > 1$, the on-site terms exhibits a pseudo-random framework. Upon a wide collection of distinct methods, it was proved that whenever the diagonal potential is bounded in a finite region $[-V, V]$ with $V < 2$, the aperiodic model contains extended states given the limit of $0 < \nu < 1$.[13,14]

The results found by Das Sarma et. al., i.e., the existence of mobility edges in 1D noncrystalline chains, stimulated other researchers to understand the role played by aperiodicity in different domains of science. In the recent years, several works involving aperiodic systems have been presented. In ref. [15], the problem of many-body localization (MBL) was experimentally investigated using ultra-cold atoms in a weak 1D quasi-periodic potential. By studying the time evolution of an initial charge density wave, a clear signature of MBL was found when the corresponding noninteracting model is tuned within the localized phase. Other system such as a bichromatic quasi-periodic optical lattice was experimentally investigated in ref. [16]. The authors found experimental evidence for the existence of a single-particle mobility edge within this system. In ref. [17], 1D mutually incommensurate bichromatic lattice system was also analyzed. This kind of system can be experimentally implemented using ultra-cold atoms framework. The authors carried out an extensive investigation of the localization properties of the 1D incommensurate lattice without making any tight-binding approximation. They obtained the existence of a localization–delocalization transition with mobility edges separating localized from extended states. It is worth mentioning that the kind of aperiodicity introduced by Das Sarma and co-workers made the treatment of the limit of strong aperiodicity ($\nu > 1$, also called pseudo-random limit) and also of the quasi-periodic case ($\nu < 1$) possible. The case $\nu = 1$ represent the Aubry–André's limit. Therefore, the aperiodic source used by Das Sarma represents a useful numerical scheme that helps on investigation of a wide range of aperiodicities. In ref. [18], the interplay between non-Hermiticity from nonreciprocal hopping and the aperiodicity was investigated. It was studied the topological transition of non-Hermitian skin effect in nonreciprocal Aubry–André models and it was obtained the exact phase diagram. The authors also proposed an electrical circuit that was used to demonstrate the transition properties. In ref. [19], the authors investigated a standard aperiodic Aubry–André model with power-law hopping (r^{-a}). For $a > 1$, the model is characterized by a hierarchy of regimes with mobility edges. For $a \leq 1$, all states remain delocalized.

More recently, the Aubry–André model and its generalizations as well as the Soukoulis–Economou model were extensively investigated in ref. [21]. The authors demonstrated that the

R. F. Dutra, D. Messias, C. V. C. Mendes, Dr. F. A. B. F. de Moura
Instituto de Física
Universidade Federal de Alagoas
Maceió, AL 57072-970, Brazil
E-mail: fidelis@fis.ufal.br

Dr. A. R. Neto
Faculdade de Economia
Administração e Contabilidade
Universidade Federal de Alagoas
57072-970 Maceió, AL, Brazil

Dr. A. R. Neto
Ministry of Economy – Special Secretariat for Finance
Esplanada dos Ministérios BL P, Braslia, DF 70297-400, Brazil

Dr. M. O. Sales
Instituto Federal do Maranhão (IFMA)
Campus São João dos Patos
rua Padre Santiago, s/n, Centro, São João dos Patos, MA 65665-000, Brazil

The ORCID identification number(s) for the author(s) of this article can be found under https://doi.org/10.1002/pssb.201900782.

DOI: 10.1002/pssb.201900782

aperiodicity plays relevant role within the context of mobility edges and also the single-particle intermediate phase. In broad strokes, the localization aspects within aperiodic systems has been investigated both theoretically and experimentally. The main results suggest that the aperiodicity promotes the appearance of extended states hence increasing the conductance.[23]

In this work, we report further progress on the subject of electronic propagation in systems with aperiodicity. We consider the electron dynamics on a square lattice in which the hopping terms follow an aperiodic distribution, and the presence of a static electric field parallel to the lattice. The source of aperiodicity here is similar to that used by Das Sarma: we assume a sinusoidal function whose phases are proportional to a power-law. The power-law exponent controls the degree of aperiodicity in the lattice. In this system, wave-packet time evolution is described by the Schrödinger equation; we solved that using a Taylor formalism. Our calculations suggest that the system may exhibit a fast electron propagation (ballistic propagation) depending on the degree of aperiodicity. When a static electric field is inserted, our calculations reveal the existence of an oscillatory behavior similar to that happen in crystalline systems(i.e., Bloch oscillations). We also investigated the frequency as well as the size of these oscillations, and compared our results with the standard semi-classical approach used in crystalline lattices.

2. Model and Formalism

We consider initially the Hamiltonian of an electronic model with aperiodic hopping energies $t_{nm,jk}$ on a rectangular $N \times N$ lattice[8,24]

$$H = \sum_{n,m} \epsilon_{n,m} |n,m\rangle\langle n,m| + \sum_{\langle im,jk\rangle} (t_{nm,jk} |n,m\rangle\langle j,k|) \tag{1}$$

where $|n,m\rangle$ is a Wannier state localized at site (n,m) and $\sum_{\langle nm,jk\rangle}$ represents a sum over nearest-neighbor pairs. In our calculations, the on-site energy $\epsilon_{n,m}$ is related to the presence of a static electric field $E = E_x x + E_y y$. The potential energy of the electron interacting with this electric field is given by: $\epsilon_{n,m} = E_x(n - N/2) + E_y(m - N/2)$ (the electron charge e and the lattice spacing a were considered $e = a = 1$[8]). To generate an aperiodic hopping energy topography, we compute the following 2D aperiodic function defined as[8,13–17]

$$\zeta_{n,m} = W \cos(\pi\alpha n^{\nu}) \cos(\pi\alpha m^{\nu}) \tag{2}$$

where W is a constant and $\pi\alpha$ is a rational number. Here, within the 2D geometry, $W < 4$.[8] The exponent ν controls the degree of aperiodicity within this 2D landscape. The hopping energy $t_{nm,jk}$ is given by $t_{nm,jk} = \exp(-|\zeta_{n,m} - \zeta_{j,k}|)$. We stress that this exponential transformation generates a bounded interval of the aperiodic variable without changing its intrinsic incommensurate properties—it is a numerical trick deployed to assure aperiodicity in the off-diagonal term's distribution without any null hopping terms. We emphasize that the choice of this kind of aperiodicity has a great advantage in comparison with other aperiodic distribution. The degree of aperiodicity within this 2D sinusoidal function can be tuned by a single parameter ν. For $\nu > 1$, we are dealing with the pseud-random limit. For $\nu < 1$, we have a quasi-periodic limit. Therefore, this procedure allows for generation of various kinds of aperiodic potentials. The Wannier amplitudes evolve in time according to the time-dependent Schrödinger equation as ($\hbar = 1$)[8,24]

$$\begin{aligned} i\frac{dc_{n,m}(t)}{dt} &= [E_x(n - N/2) + E_y(m - N/2)]c_{n,m} \\ &+ t_{nm.nm-1}c_{n,m-1}(t) + t_{nm.nm+1}c_{n,m+1}(t) \\ &+ t_{nm.n-1m}c_{n-1,m}(t) + t_{nm.n+1m}c_{n+1,m}(t) \\ i, m &= 1, 2, \ldots, N \end{aligned} \tag{3}$$

In the absence of electric field ($E_x = E_y = 0$), we considered the electron initially localized at site $n_0 = N/2, m_0 = N/2$, i.e., $|\Phi(t=0)\rangle = \sum_{n,m} c_{n,m}(t=0)|n,m\rangle$, where $c_{n,m}(t=0) = \delta_{n,n_0}\delta_{m,m_0}$. For $E_x = E_y = E > 0$, we defined the initial state as a Gaussian packet with $c_{n,m}(t=0) = (1/A)\exp(-D(n,m)^2/4)$, where $D(n,m) = \sqrt{(n-n_0)^2 + (m-m_0)^2}$ and A is a normalization constant. The aforementioned set of equations were solved numerically by using a high-order method based on the Taylor expansion of the evolution operator $V(\Delta t) = \exp(-iH\Delta t) = 1 + \sum_{l=1}^{z_o}[(-iH\Delta t)^l]/l!$, where H is the Hamiltonian. The wave-function at time Δt is given by $|\Phi(\Delta t)\rangle = V(\Delta t)|\Phi(t=0)\rangle$. The method can be used recursively to obtain the wave-function at time t. To get $H^l|\Phi(t=0)\rangle$, we used a recursive formula derived as follows. Let $H^l|\Phi(t=0)\rangle = \sum_{nm} C^l_{n,m}|n,m\rangle$. Using the Hamiltonian formula (Equation (1)), we compute $H^1|\Phi(t=0)\rangle$ and obtain $C^1_{n,m}$ as

$$\begin{aligned} C^1_{n,m} &= [E_x(n - N/2) + E_y(m - N/2)]c_{n,m}(t=0) \\ &+ t_{nm.nm-1}c_{n,m-1}(t=0) + t_{nm.nm+1}c_{n,m+1}(t=0) \\ &+ t_{nm.n-1m}c_{n-1,m}(t=0) + t_{nm.n+1m}c_{n+1,m}(t=0) \end{aligned} \tag{4}$$

Therefore, using that $H^l|\Phi(t=0)\rangle = H\sum_{nm} C^{l-1}_{n,m}|n,m\rangle$, $C^l_{n,m}$ can be obtained recursively as

$$\begin{aligned} C^l_{n,m} &= [E_x(n - N/2) + E_y(m - N/2)]C^{l-1}_{n,m} \\ &+ t_{nm.nm-1}C^{l-1}_{n,m-1} + t_{nm.nm+1}C^{l-1}_{n,m+1} \\ &+ t_{nm.n-1m}C^{l-1}_{n-1,m} + t_{nm.n+1m}C^{l-1}_{n+1,m} \end{aligned} \tag{5}$$

The results without electric field can be taken adopting $\Delta t = 0.08$ and the sum was truncated at $z_o = 10$. This cutoff was sufficient to keep the wave-function norm conservation along the entire time interval considered. In the case considering electric field, we have used $\Delta t = 0.01$ and $z_0 = 12$. This formalism is faster than high-order Runge Kutta methods and it is easier to implement. We are particularly interested in calculating the electronic mean position defined as

$$R(t) = \frac{1}{\sqrt{2}}(x + y) \cdot (\langle n\rangle(t)x + \langle m\rangle(t)y) \tag{6}$$

where $\langle n\rangle(t) = \sum_{n=1}^{N}\sum_{m=1}^{N} n|c_{n,m}(t)|^2$ and $\langle m\rangle(t) = \sum_{n=1}^{N}\sum_{m=1}^{N} m|c_{n,m}(t)|^2$. We also computed wave packet mean-square displacement $\sigma(t)$ defined by[24]

$$\sigma(t) = \sqrt{\sum_{n=1}^{N}\sum_{m=1}^{N}[(n-n_0)^2 + (m-m_0)^2]|c_{n,m}(t)|^2} \quad (7)$$

Note that $\sigma(t)$ varies from 0, for a wave function confined to a single site, to N, for a wave uniformly extended over the whole chain.[8,24,26]

3. Results

Our first analysis is carried in the case of a $N \times N$ lattice with $N = 3000$, $W = 3$ and without electric field, i.e., $E_x = E_y = 0$. Because of the system size, we did not solve the set of equations for all sites, only for a finite fraction of the lattice around the center of chain ($n_0 = N/2$ and $m_0 = N/2$). This subdivision started with size $N_0 \times N_0$ (with $N_0 = 100$) centered around the site (n_0, m_0). Whenever the wave-packet arrived at the borders of this small region, we expanded N_0 to avoid boundary effects. This artifice speeds up the calculations and also removes the possibility of border reflections. In **Figure 1**a, we plot our results for the mean square displacement σ versus t for $E_x = E_y = 0$, $\pi\alpha = 0.5$, and $\nu = 0.5, 0.75, 1.5, 2$. The results showed in Figure 1a indicated that, for $\nu < 1$, the wave-function spread increased roughly linearly with time (i.e., $\sigma(t) \propto t^1$). It is a clear signature that exists extended states at this limit. In contrast, computation for $\nu > 1$ showed that the time evolution of wave-function's width exhibited a slower dynamic pointing at the absence of extended states at this limit. To analyze the localization–delocalization transition within this model, we watch the long-time behavior of σ as the ν exponent is tuned. In broad strokes, for long times, the mean square displacement behaves as $\sigma \propto t^{\beta}$, where the exponent β depends on ν. To obtain the dependence of β with ν, we run several numerical simulations considering ν within the range $[0.1, 1.5]$. We also considered several values for the parameter $\pi\alpha$ ($\pi\alpha = 0.2$ up to 2.0). Figure 1b contains the average curve $\beta \times \nu$ obtained using all calculations. The exponent β was computed through a power-law fitting at the long-time limit. The results showed in Figure 1b indeed confirm that for $\nu < 1$ the dynamics is ballistics (i.e., the systems contains extended states). However, within our accuracy, the critical points separating extended from localized states is slightly smaller than $\nu = 1$. Based on Figure 1b, we notice that only for $\nu < 0.8$ the dynamics seems to be really ballistics. For $\nu = 0.8$, the long-time behavior of σ was characterized by an exponent $\beta = 0.97(2)$. For $\nu = 0.9$, we obtained $\beta = 0.94(2)$ and for $\nu = 1$, $\beta = 0.84(2)$. Therefore, for $0.8 \leq \nu \leq 1$, the dynamics seems to be super-diffusive with exponents between $[0.84, 0.97]$. We stress that within the 1D case studied by Das Sarma and co-workers, the critical point separating extended from localized states was $\nu = 1$. Within the framework of 2D models with nonperiodic hopping terms this general trend seems to be also roughly found; however, the critical point is slightly smaller than $\nu = 1$. In general, for $\nu < 1$, we found a fast electronic dynamics; however, only for $\nu < 0.8$, we indeed found a really ballistic propagation.

We will consider now the effect of a static electric field parallel to the aperiodic lattice (i.e., $E = E_x x + E_y y$) with $E_x = E_y = E$. We emphasize that at the presence of electric field, the wave-packet remains trapped around the initial position. Therefore, it is not necessary to consider big systems. Within the cases with electric field, we considered a $N \times N$ lattice with $N = 300$, $\pi\alpha = 0.5$, and $W = 3$. The Taylor formalism was considered with $\Delta t = 0.01$ and $z_0 = 12$. All calculations with nonzero electric field were carried for times up to $t_{max} = 2000$. For the improvement of system dynamics visualization, we plot the data for short times ($t \approx 100$). In **Figure 2** and **3**, we plot a summary of our main calculations considering $E = 0.5$ (Figure 2) and $E = 0.7$ (Figure 3). In Figure 2 and 3a,b, we plot the electronic mean position versus time for $E = 0.5$ and 0.7 considering $\nu = 0.5$ and 1.5. For $\nu = 0.5$, we could see that for both values of E, the electronic wave-packet exhibit a coherent oscillatory motion with a single frequency. For $\nu = 1.5$, we observed a complete absence of a coherent dynamics. The oscillatory dynamics found in Figure 2 and 3 for $\nu = 0.5$ is similar to the "Bloch oscillations",[8,27] originally defined within the framework of crystalline lattices. Using a semi-classical formalism,[8,27] it was easy to prove that, in a crystalline system (i.e., disorder free), an uniform

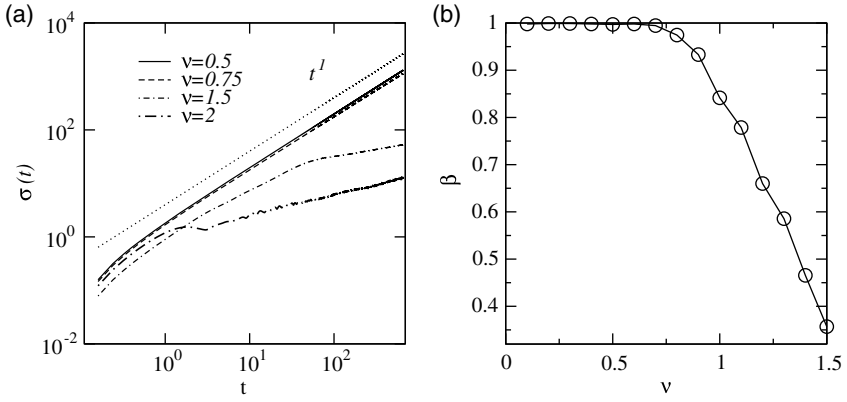

Figure 1. a) Mean square displacement σ versus t for $E_x = E_y = 0$ and $\nu = 0.5, 0.75, 1.5, 2$. Our results indicate that for $\nu < 1$ the wave-function exhibits roughly a ballistic spread (i.e., $\sigma(t) \propto t^{\beta}$ with $\beta \approx 1$). b) The exponent β versus ν considering ν within the range $[0.1, 1.5]$. Calculations of β were averaged using $\pi\alpha = 0.2$ up to 2.0.

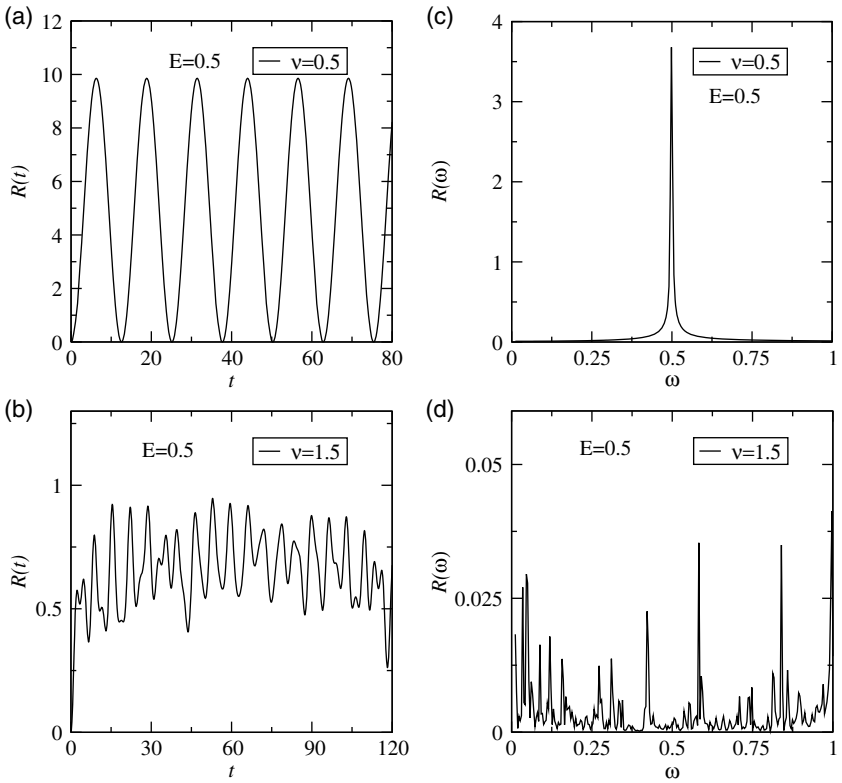

Figure 2. a,b) Electronic mean position $R(t)$ versus time for electric field $E_x = E_y = E = 0.5$ and considering $\nu = 0.5$ and 1.5. c,d) The Fourier transform $R(\omega)$ versus ω for the cases shown in (a,b).

electric field E causes dynamic localization of the wave-packet. Moreover, the interaction with the electric field also gives rise to an oscillatory motion called Bloch oscillations.[8] The semi-classical procedure also provides the frequency (ω_E) of the electronic oscillations as well as the size (L_E) of the segment over which the electron keep its dynamics: $\omega_E = E$ and $L_E \propto 1/E$ (we are considering units in which that $e = \hbar = a = 1$). We calculated the oscillation frequency using fast Fourier transform of the function $R(t)$. Our results of $R(\omega)$ versus ω for $E = 0.5, 0.7$ and $\nu = 0.5$ and 1.5 are found in Figure 2 and 3c,d. We noted that, for $\nu = 0.5$, the Fourier transform revealed a well-defined single peak around $\omega = E$ (congruent with the semi-classical predictions). For $\nu = 1.5$, we found a wide Fourier spectrum, thus indicating the total absence of a coherent Bloch oscillation. Therefore, for $0 < \nu < 1$, our results indeed suggested that the electric field promotes the appearance of "Bloch-like oscillations" with frequency in excellent agreement with the semi-classical predictions.

We analyzed other aspects related to the oscillatory behavior found in Figure 2 and 3 and its comparisons with the semi-classical predictions. In **Figure 4**a, we plot $R(t)$ versus t for $\nu = 0.5$, $\pi\alpha = 0.5$, and $E = 0.2$,0.4,0.6 and 0.8. We observed clearly that the amplitude of the oscillatory behavior decreases as the electric field intensity is increased. This results seemed to be in consonance with the semi-classical results. To make a direct comparisons, we estimated the size L_E for several values of electric field E (see Figure 4b). To estimate L_E, we considered that $\langle n \rangle(t)$ and $\langle m \rangle(t)$ are roughly identical and, therefore, the size L_E can be obtained as $L_E \approx (\sqrt{2}/2)R_{\max}$, where $R_{\max}$ is the maximum value of $R(t)$. The plot of L_E versus $1/E$ is found in Figure 4b. We could see indeed $L_E \propto 1/E$ (again, in good agreement with the semi-classical predictions). We stress that, by applying a semi-classical approach to standard Bloch system, the size L_E should be given by $L_E = B/E$, where B is the width of the Bloch band. However, our model is not a Bloch system and the "Bloch band" is not well defined here. In ref. [27], they considered a generalized approximate relation $L_E = B^*/E$, where B^* was the width of the band of extended states. Therefore, roughly, the linear fitting of the data showed in Figure 4b, provided the width of the band of extended states that exists within our model. Using a linear fitting $L_E = B^*(1/E) + a$, we obtain $B^* \approx 3$. However, we stress that it is not a precise estimation of the width of extended state's band because both the numerical estimation of L_E and equation $L_E \approx B^*/E$ contains approximations. However, despite the approximations related to the size of band, our calculations indeed suggested the existence of a band of extended states in 2D systems with weak aperiodicity ($\nu < 0.8$).

4. Conclusion

In summary, we analyzed the electronic propagation in systems with aperiodicity under effect of a static electric field. Considering electron dynamics on a square lattice with hopping terms distributed aperiodically, we investigated the time evolution of an initially localized wave-packet by using a Taylor

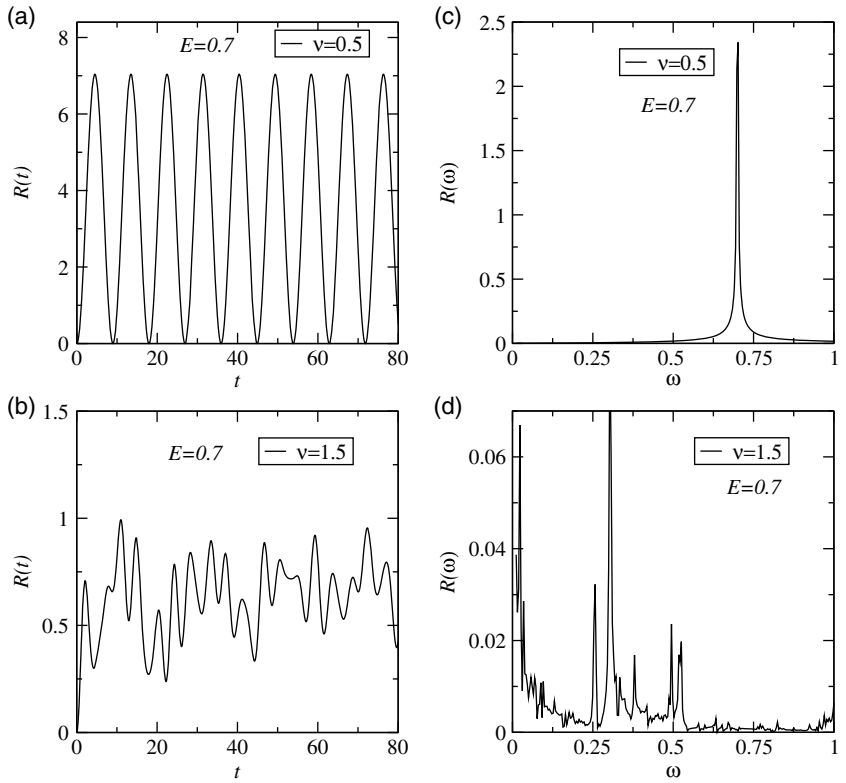

Figure 3. a,b) Electronic mean position $R(t)$ versus time for electric field $E_x = E_y = E = 0.7$ and considering $\nu = 0.5$ and 1.5. c,d) The Fourier transform $R(\omega)$ versus ω for the cases shown in (a,b).

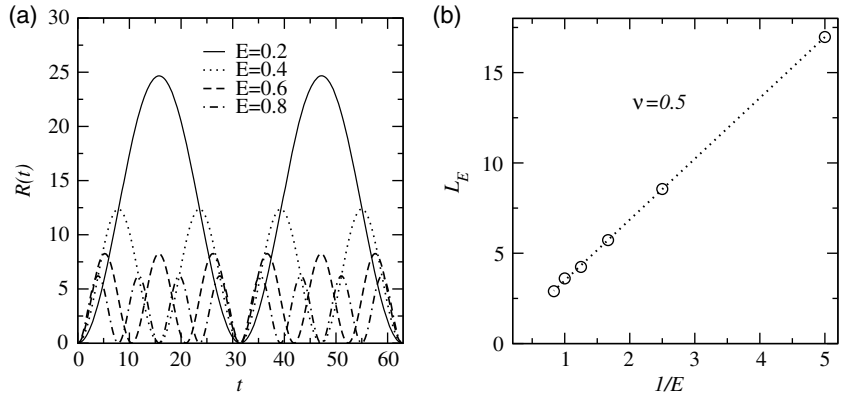

Figure 4. a) $R(t)$ versus t for $\nu = 0.5$ and $E = 0.2$, 0.4, 0.6, and 0.8. b) The size L_E versus $1/E$ considering $\nu = 0.5$.

formalism to solve the Schrödinger equation. Our results suggest that the system may exhibit a fast electron propagation (ballistic propagation) depending on the degree of aperiodicity. After introducing a static electric field to the system, our calculations revealed the existence of an oscillatory behavior which is similar to the Bloch oscillations. Also, we calculated the oscillation's frequency and the size of region in which the wave-packet remains trapped. Our results are in good agreement with the standard semi-classical approach.

Acknowledgements

The research was partially supported by the Brazilian research agencies CNPq, CAPES, INCT-Nano(Bio)Simes, as well as FAPEAL (Alagoas State Agency).

Conflict of Interest

The authors declare no conflict of interest.

Keywords

correlated disorder, diffusive spreading, localization, wave-packet dynamics

Received: December 25, 2019
Revised: March 18, 2020
Published online:

[1] E. Maciá, *Aperiodic Structures in Condensed Matter: Fundamentals and Applications*, CRC Press, Boca Raton, FL **2008**.
[2] E. Maciá, F. Domínguez-Adame, *Phys. Rev. Lett.* **1996**, *76*, 2957.
[3] E. Maciá, *Rep. Prog. Phys.* **2012**, *75*.
[4] S. Walter, D. Schneble, A. C. Durst, *Phys. Rev. A* **2010**, *81*, 033623.
[5] F. A. B. F. de Moura, M. L. Lyra, F. Domínguez-Adame, V. A. Malyshev, *Phys. Rev. B* **2005**, *71*, 104303.
[6] F. A. B. F. de Moura, L. P. Viana, A. C. Frery, *Phys. Rev. B* **2006**, *73*, 212302.
[7] A. A. Sukhorukov, *Phys. Rev. Lett.* **2006**, *96*, 113902.
[8] F. A. B. F. de Moura, L. P. Viana, M. L. Lyra, V. A. Malyshev, F. Domínguez-Adame, *Phys. Lett. A* **2008**, *372* 6694.
[9] T. Cadez, R. Mondaini, P. D. Sacramento, *Phys. Rev. B* **2017**, *96*, 144301.
[10] C. M. Dai, W. Wang, X. X. Yi, *Phys. Rev. A* **2018**, *98*, 013635.
[11] X. C. Xie, S. Das Sarma, *Phys. Rev. Lett.* **1988**, *60*, 1585.
[12] S. Das Sarma, X. C. Xie, *Phys. Rev. B* **1988**, *37*, 1097.
[13] S. Das Sarma, S. He, X. C. Xie, *Phys. Rev. Lett.* **1988**, *61*, 2144.
[14] S. Das Sarma, Song He, X. C. Xie *Phys. Rev. B* **1990**, *41*, 5544.
[15] T. Kohlert, S. Scherg, X. Li, H. P. Lüschen, S. Das Sarma, I. Bloch, M. Aidelsburger, *Phys. Rev. Lett.* **2019**, *122*, 170403.
[16] H. P. Lüschen, S. Scherg, T. Kohlert, M. Schreiber, P. Bordia, X. Li, S. Das Sarma, I. Bloch, *Phys. Rev. Lett.* **2018**, *120*, 160404.
[17] X. Li, X. Li, S. D. Sarma, *Phys. Rev. B* **2017**, *96*, 085119.
[18] H. Jiang, L.-J. Lang, C. Yang, S.-L. Zhu, S. Chen, *Phys. Rev. B* **2019**, *100*, 054301.
[19] X. Deng, S. Ray, S. Sinha, G. V. Shlyapnikov, L. Santos, *Phys. Rev. Lett.* **2019**, *123*, 025301.
[20] P. Wang, Y. Zheng, X. Chen, C. Huang, Y. V. Kartashov, L. Torner, V. V. Konotop, F. Ye, *Nature* **2020**, *577* 42.
[21] X. Li, S. D. Sarma, *Phys. Rev. B* **2020**, *101*, 064203.
[22] A. Szabó, U. Schneider, *Phys. Rev. B* **2020**, *101*, 014205.
[23] F. Flicker, J. van Wezel, *Phys. Rev. Lett.* **2015**, *115*, 236401.
[24] F. A. B. F. de Moura, M. D. Coutinho-Filho, E. P. Raposo, M. L. Lyra, *Europhys. Lett.* **2004**, *66*, 585.
[25] I. F. dos Santos, F. A. B. F. de Moura, M. L. Lyra, M. D. Coutinho-Filho, *J. Phys.: Condens. Matter* **2007**, *19*, 476213
[26] F. A. B. F. de Moura, M. L. Lyra, F. Domnguez-Adame, V. A. Malyshev, *J. Phys.: Condens. Matter* **2007**, *19*, 056204.
[27] F. Domínguez-Adame, V. A. Malyshev, F. A. B. F. de Moura, M. L. Lyra, *Phys. Rev. Lett.* **2003**, *91* 197402.